Quantum interference effects in spontaneous atomic emission: Dependence of the resonance fluorescence spectrum on the phase of the driving field

M. A. G. Martinez and P. R. Herczfeld
Electrical and Computer Engineering Department, Drexel University, Philadelphia, Pennsylvania 19104

C. Samuels and L. M. Narducci
Department of Physics, Drexel University, Philadelphia, Pennsylvania 19104

C. H. Keitel
Optics Section, Blackett Laboratory, Imperial College, London SW7 2BZ, United Kingdom
(Received 23 January 1997)

We discuss quantum interference effects in the resonance fluorescence spectrum of a Λ three-level atom when the lower-level doublet is driven by a coherent field. The interfering pathways that lead to the same final state involve both spontaneous decays and stimulated transitions, and differ from one another by an odd number of stimulated processes induced by the driving field. As a consequence, the interference structures depend upon the phase of the coherent field, an effect that is absent in other resonance fluorescence phenomena. The phase dependence of the quantum interference contribution is especially significant when the level splitting of the driven doublet is comparable to the spontaneous decay rates of the competing optical paths. [S1050-2947(97)02806-0]

PACS number(s): 42.50.Ct, 42.50.Lc, 42.50.Ar

I. INTRODUCTION

Under ideal conditions, the spectrum of the radiation emitted spontaneously by an excited atom has a Lorentzian profile with a width that scales as the Einstein A coefficient of the excited state [1]. The spectral width of the emitted radiation and, in principle, also the shape of the spectrum can be modified by placing the excited atom in a special environment, such as a high-Q resonator for example, where the density of field modes in the neighborhood of the atomic resonance can be significantly different from what is normally expected in empty space [2,3].

Because the emission spectrum is controlled by the atomic polarization fluctuations (or, more precisely, by the polarization correlation function), its shape can be modified not only by reshaping the density of vacuum modes, but also by driving the atom with a resonant or nearly resonant coherent field, as it has been common knowledge since the late 1960s and early 1970s [4–6]. Variants of the original proposals have also been suggested and demonstrated in more recent times. For example, extensions from two driven levels to three or more have included interesting complications connected with the appearance of quantum interference phenomena [7] and effects such as subnatural line narrowing [8], which are the consequence of the links (coherence) induced by the driving field(s) among the atomic states, even those that are not directly involved in the spontaneous decay process.

In general, the dynamical variables that have a most direct influence on the shape of the fluorescence spectra are the amplitudes (or, more precisely, the Rabi frequencies) and the carrier frequencies of the driving fields. This is well known. In this paper, instead, we discuss a situation where also the phase of the external field can have observable significance.

The setting of interest is illustrated schematically in Fig. 1. An atom, initially prepared in its excited state 3, can decay spontaneously to either levels 1 or 2 through dipole-allowed transitions. Levels 1 and 2, which have the same parity, are coupled to one another by an external field; for example, by a source of microwave radiation through an allowed magnetic transition.

In the absence of the driving field it is clear what to expect: as the atom decays, it generates two independent emission lines, each having a Lorentzian shape, with maxima located at the transition frequencies ω_{31} and ω_{32}, aside from small radiative shifts. When the external field is turned on, each of the two original lines splits into a doublet, as a result of the Autler-Townes effect [9]. Furthermore, the detailed shape of the fluorescence spectrum depends upon the amplitude and the carrier frequency of the driving field.

Until now, we have taken for granted that the phase of the driving field would play no role in controlling the shape of the spontaneous emission spectra. Instead, the results of our study suggest that the optical fluorescence of a driven atom can acquire an observable dependence also upon the phase of

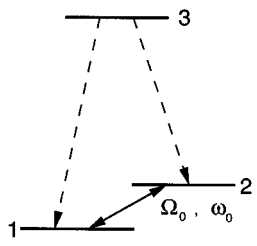

FIG. 1. Schematic representation of the relevant atomic energy levels. ω_0 and Ω_0 denote the carrier and the complex Rabi frequencies of the microwave field, respectively. The dashed lines indicate the spontaneous decay pathways; the solid line illustrates the coupling induced by the driving field.

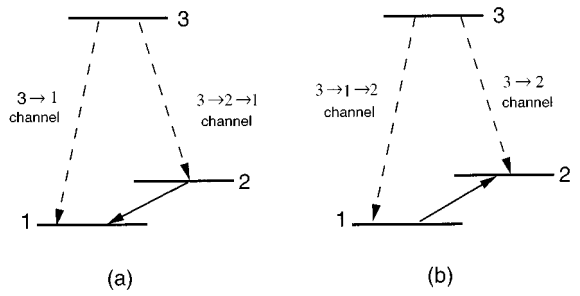

FIG. 2. Schematic representation of the first-order processes involved during the decay of an atom from level 3. (a) The two competing routes of the decay from level 3 to level 1: a direct pathway 3→1 and an indirect pathway 3→2→1, which involves the stimulated emission of a microwave photon; (b) the two routes of the decay from level 3 to level 2: a direct pathway 3→2 and an indirect pathway 3→1→2, which involves the absorption of a microwave photon.

the driving field. In fact, we predict that the spontaneous emission spectra produced by two nearly identical experimental configurations can be qualitatively different from one another, even if the only difference between the experimental setups is the presence of a phase shifter in one of the microwave beams.

While a detailed description of the model will be presented in Sec. II of this paper, it may be useful to precede the formal calculations with a qualitative description of the origin of the phase dependence. With reference to Fig. 1, we anticipate that the spectrum will consist of two main structures: one is connected with the decay of the excited electron to level 1, and the other with the decay to level 2. The two structures are spaced (from center to center) by a frequency ω_{21}, and each is split into two Autler-Townes components that are typically of unequal heights. By varying the phase of the driving field; for example, from some value φ_0 to $\varphi_0+\pi$ [10], the two Autler-Townes components switch positions. If they are of unequal heights to begin with, the new spectrum will have a different shape from the original one.

Qualitatively, we interpret this phenomenon as the consequence of two effects (see Fig. 2).

(i) The decay of the excited electron to level 1 can take place in two ways, directly from level 3 to level 1 or, indirectly, first to level 2 and then to level 1, the last step being accompanied by the stimulated emission of a microwave photon (similarly, the decay to level 2 can occur directly from the excited state or, indirectly, by way of level 1 through the subsequent absorption of a microwave photon). These two decay pathways interfere with one another and the total decay amplitude is the sum of two distinct components, as confirmed by the explicit calculations.

(ii) The indirect decay pathways, e.g., the decay 3→2→1, involve a one-photon exchange with the microwave field (a stimulated emission, in this case), while the direct decay pathway does not. Hence, the phase dependence in the fluorescence spectrum is the consequence of the interference between two decay paths, one of which depends on the complex amplitude of the driving field, while the other one does not.

The observation of the effect might begin with the preparation of a sufficient number of excited atoms and the development of a mechanism that allows them to ''see'' the same phase of the field as they begin their evolution. A reasonable way to accomplish this goal would appear to require that the atoms be excited in a time interval short enough that the field phase does not have a chance to vary appreciably. Thus, the atoms could be driven by a pulse of radiation whose duration Δt is such that the change of phase at some position within the cloud of atoms satisfies the condition $|\Delta\varphi|=\omega_0\Delta t\ll 1$, where ω_0 is the frequency of the driving field. If it should be necessary to repeat the measurement several times in order to collect an adequate spectral signal, the atoms should be prepared in their initial state with the same driving field configuration every time. Testing the predictions of our calculations does not appear to be straightforward. Nevertheless an experiment should be within reach of currently available techniques.

Our paper is organized as follows. In Sec. II we describe the model and outline the calculations leading to the fluorescence spectrum. In Sec. III we discuss specific results and offer a more detailed physical interpretation of our findings.

II. DESCRIPTION OF THE MODEL AND DERIVATION OF THE FLUORESCENCE SPECTRUM

With reference to Fig. 1, we consider a three-level atom whose excited state 3 is linked to a ground-state doublet, comprised of levels 1 and 2, by dipole-allowed transitions. The two lower states have a frequency spacing ω_{21}, and the atom is driven by a classical source of microwave radiation with a carrier frequency $\omega_0\approx\omega_{21}$ and a Rabi frequency Ω_0. Our calculation follows the procedure adopted in [11]. First, we solve the Schrödinger equation for the combined state vector of the driven atom and the radiation field; next, we construct the two-time correlation function of the radiated fluorescence; and, finally, we calculate the spectrum by taking the Fourier transform of the field correlation function.

We begin with the Schrödinger equation

$$\frac{d}{dt}|\psi(t)\rangle=-\frac{i}{\hbar}H_I(t)|\psi(t)\rangle, \tag{2.1}$$

for the combined-state vector of the atom and the surrounding electromagnetic field. The interaction Hamiltonian, in the interaction representation, is given by

$$H_I(t)=H_A+H_B(t), \tag{2.2}$$

with

$$H_A=-\hbar\delta_0 a_2^\dagger a_2+i\hbar(\Omega_0 a_2^\dagger a_1-\Omega_0^* a_1^\dagger a_2), \tag{2.3a}$$

$$H_B(t)=i\hbar\sum_k g_k(b_k a_3^\dagger a_1 e^{-i\delta_k t}-b_k^\dagger a_1^\dagger a_3 e^{i\delta_k t}) + i\hbar\sum_k g_k'(b_k a_3^\dagger a_2 e^{-i(\delta_k+\omega_0)t}-b_k^\dagger a_2^\dagger a_3 e^{i(\delta_k+\omega_0)t}). \tag{2.3b}$$

In Eqs (2.3) the symbols $a_i^\dagger$ and a_i denote the creation and annihilation operators of the atomic electron in level i ($i=1,2,3$), $b_k^\dagger$ and b_k are the corresponding operators for the

kth mode of the electromagnetic field with frequency ω_k, and g_k and g_k' are coupling constants between the kth mode of the field and the atom; g_k is associated with the $3\rightarrow1$ transition and g_k' with the $3\rightarrow2$ transition. The detuning parameters δ_0 and δ_k are defined by

$$\delta_0=\omega_0-\omega_{21}, \quad \delta_k=\omega_k-\omega_{31}, \tag{2.4}$$

respectively. The origin of the atomic energy scale is set at the lowest atomic level 1.

A convenient basis for the atomic Hilbert space consists of the unperturbed excited state $|3\rangle$ and of the dressed states $|\alpha\rangle$ and $|\beta\rangle$ resulting from the interaction of the atom with the classical microwave field. The dressed states are defined by the eigenvalue equations

$$H_A|\alpha\rangle=\hbar\lambda_\alpha|\alpha\rangle, \tag{2.5a}$$

$$H_A|\beta\rangle=\hbar\lambda_\beta|\beta\rangle, \tag{2.5b}$$

respectively, where

$$\lambda_\alpha=-\frac{\delta_0}{2}+\sqrt{\left(\frac{\delta_0}{2}\right)^2+|\Omega_0|^2}, \tag{2.6a}$$

$$\lambda_\beta=-\frac{\delta_0}{2}-\sqrt{\left(\frac{\delta_0}{2}\right)^2+|\Omega_0|^2}. \tag{2.6b}$$

Their explicit form, in terms of the unperturbed atomic states $|1\rangle$ and $|2\rangle$, is given by

$$|\alpha\rangle=\sin\theta|1\rangle+ie^{i\varphi_0}\cos\theta|2\rangle, \tag{2.7a}$$

$$|\beta\rangle=\cos\theta|1\rangle-ie^{i\varphi_0}\sin\theta|2\rangle, \tag{2.7b}$$

where

$$\sin\theta=\frac{|\Omega_0|}{\sqrt{\lambda_\alpha^2+|\Omega_0|^2}}=-\frac{\lambda_\beta}{\sqrt{\lambda_\beta^2+|\Omega_0|^2}}, \tag{2.8a}$$

$$\cos\theta=\frac{\lambda_\alpha}{\sqrt{\lambda_\alpha^2+|\Omega_0|^2}}=\frac{|\Omega_0|}{\sqrt{\lambda_\beta^2+|\Omega_0|^2}}, \tag{2.8b}$$

and

$$\Omega_0=|\Omega_0|e^{i\varphi_0}, \tag{2.9}$$

where φ_0 is defined as the phase of the driving field at the time when the atom is excited to level 3. After these preliminaries, we now seek a solution of the Schrödinger equation (2.1) in the form

$$|\psi(t)\rangle=C_3(t)|0\rangle|3\rangle+\sum_k\ [\alpha_k(t)b_k^\dagger|0\rangle|\alpha\rangle + \beta_k(t)b_k^\dagger|0\rangle|\beta\rangle], \tag{2.10}$$

subject to the initial conditions

$$C_3(0)=1, \quad \alpha_k(0)=\beta_k(0)=0. \tag{2.11}$$

In Eq. (2.10), the ket $|0\rangle$ denotes the vacuum state of the electromagnetic field.

With the help of Eqs. (2.10), (2.3), and (2.1), it is now a simple matter to derive the coupled amplitude equations

$$\frac{d}{dt}C_3(t)=\sum_k\ \{g_k[\alpha_k(t)\sin\theta+\beta_k(t)\cos\theta]e^{-i\delta_k t} + ig_k'[\alpha_k(t)\cos\theta-\beta_k(t)\sin\ \theta] \times e^{i\varphi_0}e^{-i(\delta_k+\omega_0)t}\}, \tag{2.12a}$$

$$\frac{d}{dt}\alpha_k(t)=C_3(t)[-g_ke^{i\delta_k t}\sin\theta+ig_k'e^{-i\varphi_0}e^{i(\delta_k+\omega_0)r}\cos\theta] - i\lambda_\alpha\alpha_k(t), \tag{2.12b}$$

$$\frac{d}{dt}\beta_k(t)=C_3(t)[-g_ke^{i\delta_k t}\cos\theta-ig_k'e^{-i\varphi_0}e^{i(\delta_k+\omega_0)r}\sin\theta] - i\lambda_\beta\beta_k(t), \tag{2.12c}$$

which we can solve by a method similar to the traditional Wigner-Weisskopf approach, as shown in some detail in Appendix A. For the purpose of this discussion, we only need to mention that the final result comes about after taking the infinite volume limit where the discrete index k takes on the role of a continuous variable.

Because we are interested in the structure of the fluorescence spectrum after a sufficiently long time, we only need to be concerned with the asymptotic behavior of the Schrödinger amplitudes calculated at times that are much longer than $1/\gamma$, where γ is the Einstein decay rate of level 3, given by

$$\gamma=2\pi[D(\omega_{31})g^2(\omega_{31})+D(\omega_{32})g'^2(\omega_{32})], \tag{2.13}$$

as shown in Appendix A. In Eq. (2.13) $D(\omega_x)$ represents the density of the vacuum modes calculated at the frequency ω_x, and $g(\omega_x)$ and $g'(\omega_x)$ are the corresponding coupling constants. The required amplitudes take the form

$$C_3(t\gg1/\gamma)\approx0, \tag{2.14a}$$

$$\alpha_\omega(t\gg1/\gamma)\approx e^{-i\lambda_\alpha t}\left[-g(\omega_{31})\frac{\sin\theta}{\frac{\gamma}{2}-i(\lambda_\alpha+\delta_\omega)} + ig'(\omega_{32})\frac{\cos\theta e^{-i\varphi_0}}{\frac{\gamma}{2}-i(\lambda_\alpha+\delta_\omega+\omega_0)}\right], \tag{2.14b}$$

$$\beta_\omega(t\gg1/\gamma)\approx e^{-i\lambda_\beta t}\left[-g(\omega_{31})\frac{\cos\theta}{\frac{\gamma}{2}-i(\lambda_\beta+\delta_\omega)} - ig'(\omega_{32})\frac{\sin\theta e^{-i\varphi_0}}{\frac{\gamma}{2}-i(\lambda_\beta+\delta_\omega+\omega_0)}\right], \tag{2.14c}$$

where ω is the continuous limit of ω_k, α_ω, and β_ω correspond to the discrete amplitudes α_k and β_k, respectively, and $\delta_\omega \equiv \omega - \omega_{31}$.

Now that the asymptotic form of the state vector (2.10) is known, we can calculate the spontaneous emission spectrum $S(\omega)$, which, in the continuous limit, is proportional to the Fourier transform of the field correlation function

$$\langle \vec{E}^{(-)}(\vec{r},t+\tau)\cdot\vec{E}^{(+)}(\vec{r},t)\rangle_{t\to\infty} = \langle \psi(t)|\vec{E}^{(-)}(\vec{r},t+\tau)\cdot\vec{E}^{(+)}(\vec{r},t)|\psi(t)\rangle_{t\to\infty}, \quad (2.15)$$

where

$$\vec{E}^{(+)}(\vec{r},t) = \lim_{V\to\infty} i\sum_j \left(\frac{\hbar\omega_j}{2\epsilon_0 V}\right)^{1/2} \hat{\epsilon}_j b_j e^{i(\vec{k}_j\cdot\vec{r}-\omega_j t)}, \quad (2.16a)$$

$$\vec{E}^{(-)}(\vec{r},t) = [\vec{E}^{(+)}(\vec{r},t)]^\dagger. \quad (2.16b)$$

The result of the simple calculation is

$$S(\omega) \propto |\alpha_\omega|^2 + |\beta_\omega|^2. \quad (2.17)$$

The structure of Eq. (2.17) indicates at once that quantum interference effects play a role in assigning the spectral shape of the fluorescence. In fact, both α_ω and β_ω are the sums of two separate terms, one of which [the second term in Eqs. (2.14b) and (2.14c)] depends on the phase of the driving field, while the other one does not.

If one of the decay channels, for example, the $3\to1$ pathway, could be ignored [i.e., if we set $g(\omega_{31})\approx 0$], the spectrum would no longer be sensitive to the phase of the microwave field. However, in the presence of both competing decay channels and, in particular, as a result of the interference between their transition amplitudes, the spectrum acquires a dependence upon the phase. This is the formal argument that supports the qualitative description made in the Introduction.

The main features of the spectrum (2.17) can be identified by direct inspection of Eqs. (2.14b) and (2.14c). If we consider a resonant driving field, for simplicity ($\delta_0 = 0$, $\lambda_\alpha = |\Omega_0|$, and $\lambda_\beta = -|\Omega_0|$), the spectral structure $|\alpha_\omega|^2$ is comprised of two lines centered at $\omega_{32} - |\Omega_0|$ and $\omega_{31} - |\Omega_0|$ (plus interference contributions), while $|\beta_\omega|^2$ generates lines centered at $\omega_{32} + |\Omega_0|$ and $\omega_{31} + |\Omega_0|$ (and again the interference contributions). Obviously, if $\omega_{21} > 2|\Omega_0|$ the components of $|\alpha_\omega|^2$ are interlaced with those of $|\beta_\omega|^2$; otherwise, if $\omega_{21} < 2|\Omega_0|$, the two spectral structures $|\alpha_\omega|^2$ and $|\beta_\omega|^2$ fall to the left of the unperturbed resonance ω_{32} and to the right of ω_{31}, respectively. If one should change the phase φ_0 of the driving field (a reminder: this is the phase of the field at the time when the atom is excited to level 3), the shape of the spectrum changes. In particular, if φ_0 is replaced by $\varphi_0 + \pi$, the new structure $|\alpha_\omega|^2$ is replaced by the mirror image of the old $|\beta_\omega|^2$ [12].

We can provide a complementary view of this effect if we start from a representation of the state vector that involves the unperturbed, rather than the dressed, atomic states; i.e., by replacing Eq. (2.10) with

$$|\psi(t)\rangle = C_3(t)|O\rangle|3\rangle + \sum_k [C_{1k}(t)b_k^\dagger|O\rangle|1\rangle + C_{2k}(t)b_k^\dagger|0\rangle|2\rangle], \quad (2.18)$$

where C_{1k} and C_{2k} are the probability amplitudes that the atom is found in levels 1 or 2, respectively, with a photon having been emitted in mode k. Of course there is no need to solve the problem all over again because the bare-state amplitudes C_{1k} and C_{2k} are linear combinations of the dressed amplitudes $\alpha_k(t)$ and $\beta_k(t)$, and can be calculated immediately from Eqs. (2.14) with the result

$$C_{1,\omega}(t\gg 1/\gamma) = g(\omega_{31})\left[\frac{\sin^2\theta}{\frac{\gamma}{2} - i(\lambda_\alpha + \delta_\omega)} e^{-i\lambda_\alpha t} + \frac{\cos^2\theta}{\frac{\gamma}{2} - i(\lambda_\beta + \delta_\omega)} e^{-i\lambda_\beta t}\right] + ig'(\omega_{32})e^{-i\varphi_0}\left[\frac{\sin\theta\cos\theta}{\frac{\gamma}{2} - i(\lambda_\alpha + \omega_0 + \delta_\omega)} \times e^{-i\lambda_\alpha t} - \frac{\sin\theta\cos\theta}{\frac{\gamma}{2} - i(\lambda_\beta + \omega_0 + \delta_\omega)} e^{-i\lambda_\beta t}\right], \quad (2.19a)$$

$$C_{2,\omega}(t\gg 1/\gamma) = -g'(\omega_{32})\left[\frac{\sin^2\theta}{\frac{\gamma}{2} - i(\lambda_\alpha + \omega_0 + \delta_\omega)} e^{-i\lambda_\alpha t} + \frac{\cos^2\theta}{\frac{\gamma}{2} - i(\lambda_\beta + \omega_0 + \delta_\omega)} e^{-i\lambda_\beta t}\right] - ig(\omega_{31})e^{i\varphi_0}\left[\frac{\sin\theta\cos\theta}{\frac{\gamma}{2} - i(\lambda_\alpha + \delta_\omega)} e^{-i\lambda_\alpha t} - \frac{\sin\theta\cos\theta}{\frac{\gamma}{2} - i(\lambda_\beta + \delta_\omega)} e^{-i\lambda_\beta t}\right]. \quad (2.19b)$$

A glance at the amplitudes in Eqs. (2.19) may give the impression that the fluorescence spectrum

$$S(\omega) \propto |C_{1,\omega}|^2 + |C_{2,\omega}|^2 \quad (2.20)$$

has acquired an explicit time dependence in the bare-state representation. Of course this cannot be the case, as one can verify by direct substitution of Eqs. (2.19) into Eq. (2.20) and, indeed, the result is the same as the one obtained before. Equations (2.19) show explicitly that the atom can decay, for example, to level 1 through two different pathways: one is a direct transition from the excited to the ground state, as evidenced by the appearance of the coupling constant $g(\omega_{31})$,

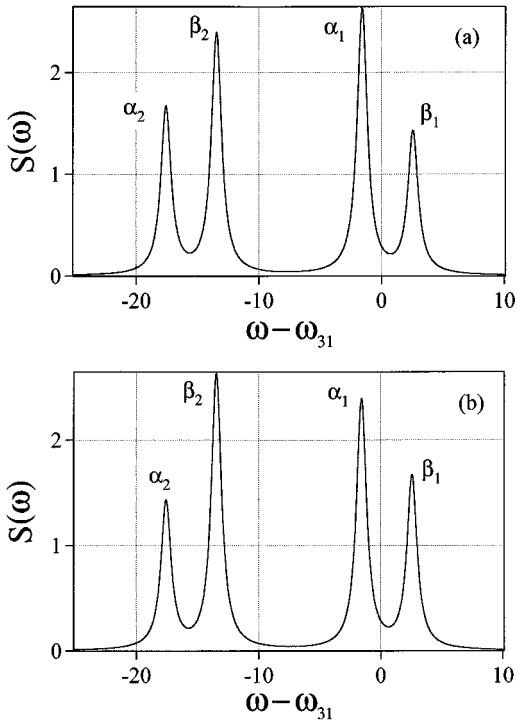

FIG. 3. (a) Spontaneous emission spectrum $S(\omega)$ in arbitrary units [see Eq. (2.17)]. The frequencies are measured in units of the Einstein rate γ [see Eq. (2.13)]. The parameters used in this simulation are $\omega_{21}=15$, $|\Omega_0|=2$, $\delta_0=1$, and $\varphi_0=0$; (b) same as (a) with $\varphi_0=\pi$. The labels α_1, α_2, β_1, and β_2 identify the doublets belonging to the structures $|\alpha_\omega|^2$ and $|\beta_\omega|^2$, respectively, as discussed in the text.

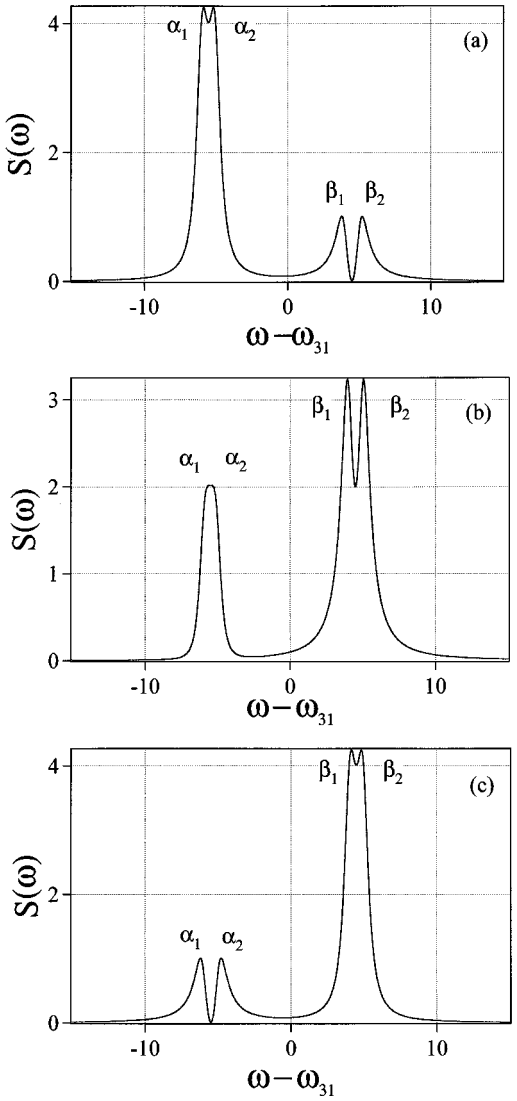

FIG. 4. (a) Spontaneous emission spectrum $S(\omega)$ in arbitrary units. The frequencies are measured in units of the Einstein rate γ [see Eq. (2.13)]. The parameters used in this simulation are $\omega_{21}=1$, $|\Omega_0|=5$, $\delta_0=0$, and $\varphi_0=0$; (b) same as (a) with $\varphi_0=\pi/2$ (in this panel the lines α_1 and α_2 are no longer resolved); (c) same as (a) with $\varphi_0=\pi$. The labels α_1, α_2, β_1, and β_2 identify the doublets belonging to the structures $|\alpha_\omega|^2$ and $|\beta_\omega|^2$, respectively, as discussed in the text.

and the other is the decay to level 2, with a weight factor $g'(\omega_{32})$, followed by the stimulated emission of a microwave photon, as indicated by the appearance of the phase factor $e^{-i\varphi_0}$. A similar interpretation can be advanced for the probability amplitude that the atom can be found in level 2, except that in this case the decay channel $3\rightarrow1\rightarrow2$ requires the absorption of a microwave photon, as indicated by the phase factor $e^{i\varphi_0}$.

Finally, as already noted, if one of the decay channels should become inaccessible [i.e., by setting either $g(\omega_{31})$ or $g'(\omega_{32})$ equal to zero] the phase dependence of the spectrum disappears, confirming that the origin of the effect lies in the quantum interference that accompanies the spontaneous emission process.

III. DESCRIPTION OF THE RESULTS AND DISCUSSION

An example of the results derived in the preceding section is shown in Figs. 3(a) and 3(b) for a case in which the microwave field is detuned from the ω_{21} resonance and the Rabi frequency $|\Omega_0|$ is small as compared to the transition frequency ω_{21}. In Fig. 3(a) the phase of the microwave field is selected as $\varphi_0=0$, while, in Fig. 3(b), φ_0 is equal to π. As anticipated in the analysis of the preceding section, the two pairs of resonances associated with each of the spectral components $|\alpha_\omega|^2$ and $|\beta_\omega|^2$ are interlaced (α_1 and α_2 in the figures belong to $|\alpha_\omega|^2$ and β_1 and β_2 to $|\beta_\omega|^2$). When the phase of the driving field is increased by π radians, the old lines α_1 and α_2 are replaced by the mirror image of the structure β_1 and β_2 (and vice versa).

If the frequency of the microwave field is resonant with the ground-state doublet, and if $g(\omega_{31})\approx g'(\omega_{32})$ (as is likely to be the case in practice because of the near degeneracy of the two lowest levels), the two lines belonging to $|\alpha_\omega|^2$ have nearly the same height, and the same is true for the components of $|\beta_\omega|^2$. In this case a phase change $\Delta\varphi_0=\pi$ modifies the fluorescence spectrum in such a way that the $|\alpha_\omega|^2$ structure is replaced by the old $|\beta_\omega|^2$, and vice versa, as shown in Figs. 4(a) and 4(c) [in Fig. 4(b) we have also shown the case $\varphi_0=\pi/2$]. In this figure we have chosen a Rabi frequency that satisfies the condition $2|\Omega_0|>\omega_{21}$ in order to display a situation where the two structures $|\alpha_\omega|^2$ and $|\beta_\omega|^2$ are located on opposite sides of the center of the entire spectrum.

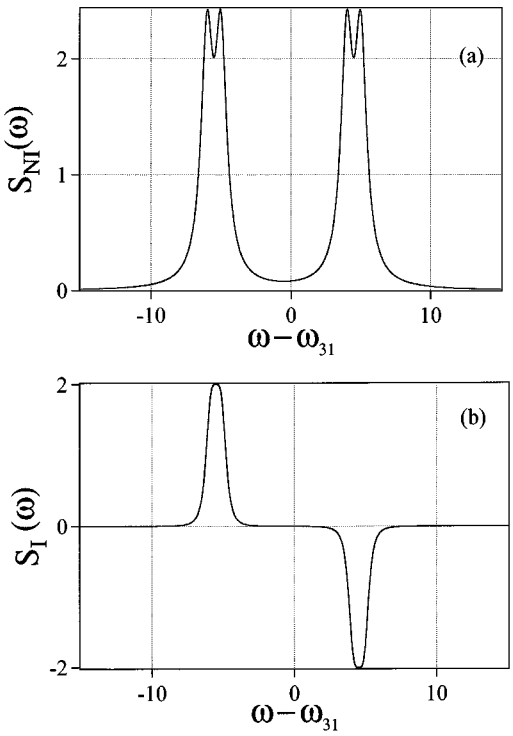

FIG. 5. (a) Noninterfering contribution to the fluorescence spectrum shown in Fig. 4(a) [see Eq. (3.1a)]; (b) interference contribution to the spectrum shown in Fig. 4(a) [See Eq. (3.1b)].

Even a glance at the results shown in Figs. 3 and 4 indicates that the phase dependence of the fluorescence spectrum can be more or less pronounced. Thus the question comes up: How can one enhance the effect of the phase dependence as much as possible? The objective of the following discussion is to argue that the optimum arrangement corresponds to a situation where the frequency spacing of the ground-state doublet ω_{21} is of the order of the decay rate γ of the excited state, although observable effects should be apparent even under less stringent conditions.

Perhaps the simplest way to address this issue is to start by writing out explicitly the fluorescence spectrum (2.17) as the sum of two parts, $S(\omega)=S_{\rm NI}(\omega)+S_1(\omega)$. The first, labeled $S_{\rm NI}$, or noninterfering contribution for convenience, is given by

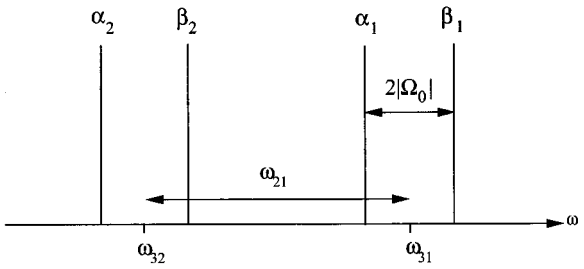

FIG. 6. Schematic representation of the spectral lines for the case $\omega_{21}>2|\Omega_0|$. α_1 and α_2 denote the two components of the $|\alpha_\omega|^2$ structure, with centers at frequencies ω_1^α and ω_2^α, respectively. β_1 and β_2 are the corresponding components of the $|\beta_\omega|^2$ structure with center frequencies at ω_1^β and ω_2^β.

$$S_{\rm NI}(\omega)=g^2(\omega_{31})\left[\frac{\sin^2\theta}{(D_1^\alpha)^2}+\frac{\cos^2\theta}{(D_1^\beta)^2}\right]+g'^2(\omega_{32})\left[\frac{\cos^2\theta}{(D_2^\alpha)^2}+\frac{\sin^2\theta}{(D_2^\beta)^2}\right]. \tag{3.1a}$$

The second, S_I, or interference contribution, is given by

$$S_I(\omega)=2g(\omega_{31})g'(\omega_{32})\sin\theta\,\cos\theta\left[-\frac{\sin(\varphi_0+\varphi^\alpha)}{D_1^\alpha D_2^\alpha}+\frac{\sin(\varphi_0+\varphi^\beta)}{D_1^\beta D_2^\beta}\right]. \tag{3.1b}$$

In Eqs. (3.1) we have introduced the symbols

$$D_1^x=\sqrt{(\gamma/2)^2+(\omega-\omega_{31}+\lambda_x)^2}, \tag{3.2a}$$

$$D_2^x=\sqrt{(\gamma/2)^2+(\omega-\omega_{31}+\omega_0+\lambda_x)^2}, \tag{3.2b}$$

and

TABLE I. Explicit expressions for the quantities D_1^x, D_2^x, and φ^x [$x=\alpha,\beta$; see Eqs. (3.2)], for $\omega=\omega_1^\alpha$, and $\omega=\omega_2^\alpha$.

	$\omega_1^\alpha=\omega_{31}-\lvert\Omega_0\rvert$	$\omega_2^\alpha=\omega_{32}-\lvert\Omega_0\rvert$
D_1^α	$\gamma/2$	$[(\gamma/2)^2+\omega_{21}^2]^{1/2}$
D_2^α	$[(\gamma/2)^2+\omega_{21}^2]^{1/2}$	$\gamma/2$
D_1^β	$[(\gamma/2)^2+4\lvert\Omega_0\rvert^2]^{1/2}$	$[(\gamma/2)^2+(\omega_{21}+2\lvert\Omega_0\rvert)^2]^{1/2}$
D_2^β	$[(\gamma/2)^2+(\omega_{21}-2\lvert\Omega_0\rvert)^2]^{1/2}$	$[(\gamma/2)^2+4\lvert\Omega_0\rvert^2]^{1/2}$
φ^α	$\arg(\gamma/2-i\omega_{21})$	$\arg(\gamma/2-i\omega_{21})$
φ^β	$-\arg\left[\frac{\gamma}{2}+i(\omega_{21}-2\lvert\Omega_0\rvert)\right]-\arg\left(\frac{\gamma}{2}+2i\lvert\Omega_0\rvert\right)$	$-\arg\left[\frac{\gamma}{2}+i(\omega_{21}+2\lvert\Omega_0\rvert)\right]+\arg\left(\frac{\gamma}{2}+2i\lvert\Omega_0\rvert\right)$

$$\varphi^x = \arg[\gamma/2 - i(\omega - \omega_{31} + \omega_0 + \lambda_x)] - \arg[\gamma/2 - i(\omega - \omega_{31} + \lambda_x)], \tag{3.2c}$$

and the superscript x stands for either α or β. The contribution $S_{\mathrm{NI}}(\omega)$ is positive definite, as expected, and it consists of the sum of four Lorentzian lines [see Fig. 5(a)]. $S_I(\omega)$, instead, is not positive definite [see Fig. 5(b)], so that some parts of the spectrum are enhanced, relative to $S_{\mathrm{NI}}(\omega)$, and others are lowered in height.

In order to avoid unnecessary algebraic complications, we now continue our discussion in the case when the driving field is resonant with the $1\rightarrow 2$ transition (i.e., $\omega_0 = \omega_{21}$). In this situation, as shown schematically in Fig. 6, the four Lorentzian lines associated with $S_{\mathrm{NI}}(\omega)$ [Eq. (3.1a)] are centered at the frequencies

$$\omega_1^\alpha = \omega_{31} - |\Omega_0|, \quad \omega_2^\alpha = \omega_{32} - |\Omega_0| = \omega_{31} - \omega_{21} - |\Omega_0|,$$
$$\omega_1^\beta = \omega_{31} + |\Omega_0|, \quad \omega_2^\beta = \omega_{32} + |\Omega_0| = \omega_{31} - \omega_{21} + |\Omega_0|. \tag{3.3}$$

If $g(\omega_{31}) \approx g'(\omega_{32})$, a straightforward analysis of Eq. (3.1a), yields the following symmetry relations (see Appendix B for some useful formulas)

$$S_{\mathrm{NI}}(\omega_1^\alpha) = S_{\mathrm{NI}}(\omega_2^\beta), \tag{3.4a}$$

$$S_{\mathrm{NI}}(\omega_2^\alpha) = S_{\mathrm{NI}}(\omega_1^\beta). \tag{3.4b}$$

For arbitrary values of the coupling constants, instead, the interference contribution of the spectrum obeys the symmetry relations

$$S_I(\omega_1^\alpha) = -S_I(\omega_2^\beta), \tag{3.5a}$$

$$S_I(\omega_2^\alpha) = -S_I(\omega_1^\beta). \tag{3.5b}$$

Thus the peak heights of the lines centered at ω_1^α and ω_2^β (the α_1 and β_2 lines in Fig. 6) are modified by the same amount, but in opposite directions, by the effect of the quantum interference [the same conclusion holds for the pair of lines centered at ω_2^α and ω_1^β (the α_2 and β_1 lines in Fig. 6)]. As we have already stated, a phase change $\varphi_0 \rightarrow \varphi_0 + \pi$ causes the old line ω_1^α to be replaced by the old line ω_2^β (and vice versa), so that a good figure of merit for the observability of the spectral phase dependence is provided by the absolute value of the ratio $S_I(\omega)/S_{\mathrm{NI}}(\omega)$, calculated at any of the four line centers.

With reference to the ω_1^α line, for example, Eqs. (3.1) yield

$$S_{\mathrm{NI}}(\omega_1^\alpha) = \tfrac{1}{2} g^2(\omega_{31}) \left(\frac{1}{(\gamma/2)^2} + \frac{1}{(\gamma/2)^2 + 4|\Omega_0|^2} \right) + \tfrac{1}{2} g'^2(\omega_{32}) \left(\frac{1}{(\gamma/2)^2 + \omega_{21}^2} + \frac{1}{(\gamma/2)^2 + (\omega_{21} - 2|\Omega_0|)^2} \right) \tag{3.6a}$$

and

$$S_I(\omega_1^\alpha) = g(\omega_{31}) g'(\omega_{32}) \left\{ -\frac{\sin[\varphi_0 + \varphi^\alpha(\omega_1^\alpha)]}{\frac{\gamma}{2}\sqrt{(\gamma/2)^2 + \omega_{21}^2}} + \frac{\sin[\varphi_0 + \varphi^\beta(\omega_1^\alpha)]}{\sqrt{(\gamma/2)^2 + 4|\Omega_0|^2}\sqrt{(\gamma/2)^2 + (\omega_{21} - 2|\Omega_0|)^2}} \right\}, \tag{3.6b}$$

where

$$\varphi^\alpha(\omega_1^\alpha) = \arg\left(\frac{\gamma}{2} - i\omega_{21} \right), \tag{3.7a}$$

$$\varphi^\beta(\omega_1^\alpha) = \arg\left[\frac{\gamma}{2} - i(\omega_{21} - 2|\Omega_0|) \right] - \arg\left(\frac{\gamma}{2} + 2i|\Omega_0| \right). \tag{3.7b}$$

In the specific, and probably fairly common, case in which

$$\omega_{21} \gg |\Omega_0| \gg \gamma, \tag{3.8}$$

the ''visibility ratio'' scales as

$$\left| \frac{S_I(\omega_1^\alpha)}{S_{\mathrm{NI}}(\omega_1^\alpha)} \right| = O(\gamma/\omega_{21}). \tag{3.9}$$

If, instead,

$$\omega_{21} \approx \gamma \ll |\Omega_0|, \tag{3.10}$$

Eq. (3.9) is replaced by

$$\left| \frac{S_I(\omega_1^\alpha)}{S_{\mathrm{NI}}(\omega_1^\alpha)} \right| = O(1). \tag{3.11}$$

Thus, as one might expect, the effects of quantum interference are most pronounced when the transition frequency ω_{21} is of the order of the Einstein rate γ. Intuitively, this is a reasonable result because, in this limit, the two optical photons at frequencies ω_{31} and ω_{32} become virtually indistinguishable from each other.

ACKNOWLEDGMENTS

We are indebted to Professor Howard J. Carmichael and Professor Girish S. Agarwal for extensive and very useful discussions, and to Professor Sudhakar Prasad for insightful observations and comments. CHK's partial support was provided by the UK Engineering and Physical Sciences Research Council, and by the European Community Science Programme. M.A.G.M. is grateful to the Brazilian Research Council (CNPq), for partial support of this research.

APPENDIX A

The purpose of this appendix is to sketch the solution of the coupled amplitude equations (2.12) following a straightforward generalization of the Weisskopf-Wigner procedure

TABLE II. Explicit expressions for the quantities D_1^x, D_2^x, and φ^x [$x=\alpha,\beta$; see Eqs. (3.2)], for $\omega=\omega_1^\beta$, and $\omega=\omega_2^\beta$.

	$\omega_1^\beta=\omega_{31}+\lvert\Omega_0\rvert$	$\omega_2^\beta=\omega_{32}+\lvert\Omega_0\rvert$
D_1^α	$[(\gamma/2)^2+4\lvert\Omega_0\rvert^2]^{1/2}$	$[(\gamma/2)^2+(\omega_{21}-2\lvert\Omega_0\rvert)^2]^{1/2}$
D_2^α	$[(\gamma/2)^2+(\omega_{21}+2\lvert\Omega_0\rvert)^2]^{1/2}$	$[(\gamma/2)^2+4\lvert\Omega_0\rvert^2]^{1/2}$
D_1^β	$\gamma/2$	$[(\gamma/2)^2+\omega_{21}^2]^{1/2}$
D_2^β	$[(\gamma/2)^2+\omega_{21}^2]^{1/2}$	$\gamma/2$
φ^α	$-\arg\left[\frac{\gamma}{2}+i(\omega_{21}+2\lvert\Omega_0\rvert)\right]+\arg\left(\frac{\gamma}{2}+2i\lvert\Omega_0\rvert\right)$	$\arg\left[\frac{\gamma}{2}-i(\omega_{21}-2\lvert\Omega_0\rvert)\right]-\arg\left(\frac{\gamma}{2}+2i\lvert\Omega_0\rvert\right)$
φ^β	$\arg\left(\frac{\gamma}{2}-i\omega_{21}\right)$	$\arg\left(\frac{\gamma}{2}-i\omega_{21}\right)$

[1]. We start by deriving explicit formal solutions of Eqs. (2.12b) and (2.12c), with the results

$$\alpha_k(t)=\alpha_k(0)e^{-i\lambda_\alpha t}+\int_0^t dt'\ C_3(t')e^{-i\lambda_\alpha(t-t')}\times[-g_k\sin\theta e^{i\delta_k t'}+ig_k'\cos\theta e^{-i\varphi_0}e^{i(\delta_k+\omega_0)t'}], \tag{A1a}$$

$$\beta_k(t)=\beta_k(0)e^{-i\lambda_\beta t}+\int_0^t dt'\ C_3(t')e^{-i\lambda_\beta(t-t')}\times[-g_k\cos\theta e^{i\delta_k t'}-ig_k'\sin\theta e^{-i\varphi_0}e^{i(\delta_k+\omega_0)t'}]. \tag{A1b}$$

After imposing the initial conditions (2.11), substitution of Eqs. (A.1) into Eq. (2.12a) yields

$$\frac{dC_3(t)}{dt}=-\sum_{n=1}^4\left[\sum_k f_{n,k}(\omega_0,\varphi_0,t)\times\int_0^t dt'\ C_3(t')e^{-i(\omega_k-\Omega_n)(t-t')}\right], \tag{A2}$$

where

$$\Omega_1=\omega_{31}-\lambda_\alpha,\quad \Omega_2=\omega_{31}-\lambda_\beta,\quad \Omega_3=\omega_{31}-\lambda_\alpha-\omega_0,\quad \Omega_4=\omega_{31}-\lambda_\beta-\omega_0, \tag{A3}$$

and

$$f_{1,k}(\omega_0,\varphi_0,t)=g_k^2\sin^2\theta+ig_kg_k'e^{-i(\omega_0t-\varphi_0)}\sin\theta\cos\theta, \tag{A4a}$$

$$f_{2,k}(\omega_0,\varphi_0,t)=g_k^2\cos^2\theta-ig_kg_k'e^{-i(\omega_0t-\varphi_0)}\sin\theta\cos\theta, \tag{A4b}$$

$$f_{3,k}(\omega_0,\varphi_0,t)=g_k'^2\cos^2\theta-ig_kg_k'e^{i(\omega_0t-\varphi_0)}\sin\theta\cos\theta, \tag{A4c}$$

$$f_{4,k}(\omega_0,\varphi_0,t)=g_k'^2\sin^2\theta+ig_kg_k'e^{i(\omega_0t-\varphi_0)}\sin\theta\cos\theta. \tag{A4d}$$

Next, we solve Eq. (A.2) along the lines of the traditional approach of Weisskopf and Wigner, with the result

$$\frac{dC_3(t)}{dt}\approx-C_3(t)\pi\sum_{n=1}^4\left[\sum_k f_{n,k}(\omega_0,\varphi_0,t)\,\delta(\omega_k-\Omega_n)\right]. \tag{A5}$$

In the infinite volume limit we have, for example,

$$\sum_k g_k^2\delta(\omega_k-\Omega_n)\to\int d\omega_k D(\omega_k)g^2(\omega_k)\,\delta(\omega_k-\Omega_n), \tag{A6}$$

where $D(\omega_k)$ is the density of vacuum modes of the electromagnetic field, and Eq. (A.5) takes the form

$$\begin{aligned}\frac{dC_3(t)}{dt}=&-C_3(t)\pi\{[g^2(\Omega_1)\sin^2\theta+ig(\Omega_1)g'(\Omega_1)e^{-i(\omega_0t-\varphi_0)}\sin\theta\cos\theta]D(\Omega_1)\\&+[g^2(\Omega_2)\cos^2\theta-ig(\Omega_2)g'(\Omega_2)e^{-i(\omega_0t-\varphi_0)}\sin\theta\cos\theta]D(\Omega_2)\\&+[g'^2(\Omega_3)\cos^2\theta-ig(\Omega_3)g'(\Omega_3)e^{i(\omega_0t-\varphi_0)}\sin\theta\cos\theta]D(\Omega_3)+[g'^2(\Omega_4)\sin^2\theta\\&+ig(\Omega_4)g'(\Omega_4)e^{i(\omega_0t-\varphi_0)}\sin\theta\cos\theta]D(\Omega_4)\}.\end{aligned} \tag{A7}$$

In view of the weak frequency dependence of the functions g, g', and D, we can safely assume

$$g(\Omega_1)\sqrt{D(\Omega_1)}\approx g(\Omega_2)\sqrt{D(\Omega_2)}=g(\omega_{31})\sqrt{D(\omega_{31})}, \tag{A8a}$$

$$g(\Omega_3)\sqrt{D(\Omega_3)}\approx g(\Omega_4)\sqrt{D(\Omega_4)} = g(\omega_{31}-\omega_0)\sqrt{D(\omega_{31}-\omega_0)}, \tag{A8b}$$

and similar relations for g'. Thus we have

$$\frac{dC_3(t)}{dt}=-\tfrac{1}{2}\gamma C_3(t), \tag{A9}$$

where

$$\gamma=2\pi[g^2(\omega_{31})D(\omega_{31})+g'^2(\omega_{31}-\omega_0)D(\omega_{31}-\omega_0)]. \tag{A10}$$

After replacing $C_3(t')$ on the right-hand side of Eqs. (A1) with the solution of Eq. (A9), and carrying out the elementary integration, Eqs. (2.14b) and (2.14c) follow, in the long-time and infinite volume limits.

APPENDIX B

For the convenience of the reader, we list in Tables I and II a number of formulas that will allow a verification of Eqs. (3.4) and (3.5) virtually by inspection (note: on resonance we have $\sin\theta=\cos\theta=1/\sqrt{2}$).

[1] V. Weisskopf and E. Wigner, Z. Phys. **63**, 54 (1930); **65**, 18 (1931).

[2] E. M. Purcell, Phys. Rev. **69**, 681 (1946).

[3] D. Kleppner, Phys. Rev. Lett. **47**, 232 (1981); S. Haroche and D. Kleppner, Phys. Today **42** (1), 24 (1989).

[4] A. I. Burshtein, Sov. Phys. JETP **22**, 939 (1966); M. C. Newstein, Phys. Rev. **167**, 89 (1968).

[5] B. R. Mollow, Phys. Rev. **188**, 1969 (1969); Phys. Rev. A **2**, 76 (1970).

[6] W. Hartig and H. Walther, Appl. Phys. **1**, 171 (1973); F. Shuda, C. R. Stroud, Jr., and M. Hercher, J. Phys. B **7**, L198 (1974); F. Y. Wu, R. E. Grove, and S. Ezekiel, Phys. Rev. Lett. **35**, 1426 (1975); R. E. Grove, F. Y. Wu, and S. Ezekiel, Phys. Rev. A **15**, 227 (1975).

[7] See, for example, G. Alzetta, A. Gozzini, L. Moi, and G. Orriols, Nuovo Cimento B **36**, 5 (1976); C. Cohen-Tannoudji and S. Reynaud, J. Phys. B **10**, 345 (1977); **10**, 365 (1977); **10**, 2311 (1977); H. R. Gray, R. M. Whitley, and C. R. Stroud, Jr., Opt. Lett. **3**, 218 (1978); P. L. Knight, J. Phys. B **12**, 3297 (1979); D. Agassi, Phys. Rev. A **30**, 2449 (1984); P. M. Radmore, S. Tarzi, and P. L. Knight, J. Mod. Opt. **34**, 587 (1987).

[8] L. M. Narducci, M. O. Scully, G.-L. Oppo, P. Ru, and J. R. Tredicce, Phys. Rev. A **42**, 1630 (1990); D. J. Gauthier, Y. Zhu, and T. W. Mossberg, Phys. Rev. Lett. **66**, 2460 (1991); C. H. Keitel, L. M. Narducci, and M. O. Scully, Appl. Phys. B **60**, 153 (1995).

[9] S. H. Autler and C. H. Townes, Phys. Rev. **100**, 703 (1955).

[10] When we mention a given phase of the driving field φ_0, for example, we refer to the phase of the field at the time when the atoms are excited and the evolution of the system is about to begin.

[11] Shi-Yao Zhu, Lorenzo M. Narducci, and Marlan O. Scully, Phys. Rev. A **52**, 4791 (1995).

[12] To be more precise, a gradual change in φ_0 leads to a gradual change in the shape of both $|\alpha_\omega|^2$ and $|\beta_\omega|^2$, but not in the position of the resonances on the frequency axis. When the phase acquires the value $\varphi_0+\pi$, the new spectral shape $|\alpha_\omega|^2$ matches the mirror image of the old $|\beta_\omega|^2$ and vice versa.